Marine Biodiversity (2025) 55:15
https://doi.org/10.1007/s12526-024-01493-x

SENCKENBERG

ORIGINAL PAPER

Going deep into *Parazoanthus axinellae* (Anthozoa: Zoantharia) complex: description of two species in the Alboran Sea based on an integrative approach

Alfredo Rosales Ruiz[1,2] · Oscar Ocaña[2] · Roberto de la Herrán[1] · Rafael Navajas-Pérez[1] · Carmelo Ruiz Rejón[1] · Ander Congil Ross[2] · Francisca Robles[1]

Received: 28 March 2024 / Revised: 2 December 2024 / Accepted: 3 December 2024

Abstract

Parazoanthus axinellae Schmidt, 1862 (Anthozoa: Zoantharia) has been historically divided into different taxa at various levels (varieties, morphotypes, or subspecies) and is considered a species complex by some authors. This species has a wide distribution, is a key part of coralligenous habitats, and constitutes one of the main ecosystems in the Alboran and Mediterranean Seas. In this work, we propose the reclassification of one subspecies and a new species of *Parazoanthus*: *Parazoanthus brevitentacularis* stat. nov. and *Parazoanthus franciscae* sp. nov. The first was described as a morphotype (named "stocky") and as the subspecies *P. axinellae brevitentacularis*, while the second is described here for the first time. An integrative approach, combining morphological, ecological, histological, and genetic analyses, allowed us to detect enough variability to establish this new species and led us to better understand the diversity of this group. Morphological and ecological analyses have been performed in situ by observing the main different features of the species. Histological examinations to propose the systematics of the species and the main diagnostic characters to identify them were performed based on the macro-anatomy, micro-anatomy, and the features of the cnidome. Genetic analyses were performed using common molecular markers (*COI* and *ITS*) and mitochondrial genome sequencing (MGS). The *COI* region was limited in establishing informative relationships within the species. MGS was a powerful tool to assess diversity, although somewhat limited due to the small number of genome sequences available, and the slow evolution of mitochondrial genomes in Anthozoa. Ribosomal *ITS* showed wider distances between taxa, resulting in the phylogenetic trees being most congruent with the ecological, morphological, and histological analyses.

Keywords Taxonomy · Corals · Phylogenetic · Diversity · Morphotypes

Introduction

Traditionally, Zoantharia species have been classified based on morphological characters such as the cnidome or the sphincter anatomy (Pax 1937a; Pax b; Pax 1957; Abel 2959; Gili et al. 1987; Ryland and Lancaster 2004; Ocaña and Brito 2004; Costa et al. 2011; Ocaña and Çinar 2018). In recent years, an increasing number of molecular phylogenetic techniques based on nucleotide sequences have been applied on zoantharians, usually complemented by morphological analyses (Sinniger et al. 2005, 2008, 2010, 2013; Reimer et al. 2006; Reimer and Todd 2009; Sinniger and Häussermann 2009; Chen et al. 2009; Reimer and Fujii 2010; Fujii and Reimer 2013; Swain and Swain 2014; Cachet et al. 2015; Santos et al. 2016; Carreiro-Silva et al. 2017; Swain 2018; Kise et al. 2018, 2021; Villamor et al. 2020).

Communicated by Danwei Huang

This article is registered in ZooBank under https://zoobank.org/BA10008F-87F0-4F5B-B5B6-03177E840BE7

✉ Alfredo Rosales Ruiz
alfredrosales@correo.ugr.es

✉ Roberto de la Herrán
rherran@ugr.es

[1] Department of Genetics, University of Granada, Granada, Spain

[2] Fundacion Museo del Mar de Ceuta, Ceuta, Spain

Published online: 08 February 2025

Molecular phylogenies have been frequently reconstructed using a portion of the mitochondrial cytochrome oxidase subunit I gene (*COI*) (Hebert et al. 2003), or in combination with other genomic regions (Swain 2018). However, the efficiency of this method has been previously questioned in this group of species (Sinniger et al. 2008; Krishna Krishnamurthy and Francis 2012). In anthozoans, mitochondrial genomes have been shown to evolve five times slower than nuclear sequences (Chen et al. 2009) and 50–100 times slower than mitochondrial genomes from other metazoans, resulting in low levels of interspecific variation in corals, even when nuclear loci show high variations (Hellberg 2006; Huang et al. 2008). Although the use of these regions has been deeply debated, especially during the early years of the proposed method based on the barcoding regions (France and Hoover 2002; Shearer et al. 2002; Fukami and Knowlton 2005; Concepcion et al. 2006; Huang et al. 2008; McFadden et al. 2011; Dohna and Kochzius 2016), they have been useful when constructing phylogenetic relationships within families, genera, and species of the order Zoantharia using these mitochondrial sequences alone (Sinniger et al. 2005, 2008) or in combination with nuclear variable regions such as ribosomal internal transcribed spacers (*ITS*) (Sinniger and Häussermann 2009; Sinniger et al. 2010; Fujii and Reimer 2011, 2013; Santos et al. 2016; Carreiro-Silva et al. 2017; Swain 2018; Montenegro et al. 2020; Kise et al. 2021, 2023). Recently, new methods, such as the use of whole mitochondrial genome analyses, RAD-Seq, and the use of new mitochondrial regions, have deepened our understanding of the taxonomic relations among anthozoan groups (Poliseno et al. 2020; Quattrini et al. 2022; Ramírez-Portilla et al. 2022).

Within the order Zoantharia, the family Parazoanthidae sensu lato contains 16 recognized genera (Reimer and Sinniger 2024). The largest genus, *Parazoanthus* Haddon and Shackleton (1891), comprises 16 accepted species distributed worldwide and is present in a large variety of habitats (Sinniger et al. 2010). In the Mediterranean, the most common species of Zoantharia growing on rocky substrate with an extensive bathymetric range is *Parazoanthus axinellae* Schmidt, 1862. The species was first described in the Adriatic (Schmidt 1862), later revisited in the Adriatic by Pax (1937a, b, and 1957), and cited in the Gulf of Naples by Abel (1959), in the northern area of the Gulf of Lion by Herberts (1972), in the Catalonia coast by Gili et al. (1987), and in the Alboran Sea by Ocaña et al. (2000). This species, which could be treated as a species complex, has been historically divided into four subspecies, *Parazoanthus axinellae adriaticus* Pax, 1937, *Parazoanthus axinellae mülleri* Pax, 1957, *Parazoanthus axinellae liguricus* Pax, 1937, and *Parazoanthus axinellae brevitentacularis* Abel, 1959. These were merged into two different morphotypes by Cachet et al. (2015) and, most recently, by Ocaña et al. (2019). The first one includes *P. axinellae brevitentacularis*, cited as morphotype "stocky" or "morphotype 1," and the second one includes the three subspecies remaining, as morphotype "slender" or "morphotype 2" (Cachet et al. 2015; Ocaña et al. 2019; Villamor et al. 2020), being both present in the Alboran sea (Ocaña et al. 2019; Villamor et al. 2020).

P. axinellae brevitentacularis shows important differences in ecology and color in relation to other morphotypes, grows over the sponge *Petrosia* spp., and more commonly over rocky walls. It has an invariable orange column normally with a few incrusted mineral particles in the ectoderm, and the disc is also orange with evident radiae and thickening, especially along the second cycle of tentacles. Populations are related to rheophilic habitats, forming large concentrations of polyps from 1 to 40 m, but in contrast to other morphotypes of *P. axinellae*, they have not been observed growing on *Axinella* spp. It has been detected in the Occidental Mediterranean Basin and in Macaronesian Archipelagos (Ocaña et al. 2019). Molecular studies conducted on this morphotype using metabolomic techniques (Cachet et al. 2015), COI and ITS sequences polymorphisms (Villamor et al. 2020), or SNPs by 2bRAD (Terzin et al. 2024) have revealed divergences between this and other morphs. These differences were also confirmed through morphological and ecological features (Ocaña et al. 2019). As a result, authors have proposed it as an independent taxon (Ocaña et al. 2019; Terzin et al. 2024), although it has not yet been described as a distinct species due to the necessity for additional molecular analysis and a precise morphological description, which will both be performed in the present work.

The morphotype "slender" includes different varieties of yellowish *P. axinellae* sensu lato specimens, growing almost exclusively on *Axinella* spp., but also found over rocky substrates from 5 to 80 m. The column is completely covered by incrusted mineral particles, forming a thick layer. Tentacles and a nearby disc portion are pale yellow, with an orange disc center and hypostome, column pinkish or yellowish throughout, although whitish near the tentacles (Ocaña et al. 2019). It has a wide distribution, being present along the Mediterranean and Northeast Atlantic coasts (Villamor et al. 2020; Terzin et al. 2024). This morph is perhaps the most variable and could be polyphyletic.

In this study, we use an integrative method based on ecological and macrostructural observations, morphological analysis of the cnidome, COI, ITS regions, and whole mitochondrial genome analysis to resolve the classification of the *P. axinellae* species complex, specifically "slender," "stocky," and a newly observed morphotype, testing the main hypothesis of independence among these three taxa.

Material and methods

Specimen collection and preparation

Three *Parazoanthus* morphotypes were observed in the Alboran Sea in different underwater transects conducted by ROV (Nido Robotics Sibiu Pro) and SCUBA diving during 2021 and 2022. Samples were collected by SCUBA in Calahonda-Castell de Ferro Special Area of Conservation (SAC), Granada, Spain; Punta de la Mona SAC, Granada, Spain; Maro-Cerro Gordo Reserve, Granada, Spain; Chafarinas Islands SAC; and Monte Hacho Site of Community Importance (SCI), Ceuta, Spain (Table S1). Firstly, habitats and specimens were photographed using an Olympus TG-6 compact underwater camera. Colonies of 8–12 polyps were kept underwater in separate bags, taking special care not to mix morphotypes during the process. Soon after arriving at the shore, half the polyps of each sample were fixed in an 8% seawater-formaldehyde solution and later stored in 70% alcohol. The other half of the samples were preserved using 80% ethanol, refrigerated at 12 °C in a cooler, and then stored at 4 °C in the laboratory for further analysis. Samples were stored and preserved in the Museo del Mar de Ceuta (MMC) collection.

Morphological analyses

The morphology and anatomy were studied on formalin-preserved samples using a stereo-dissecting microscope. The anatomical and micro-anatomical details were studied using staining *in toto*, following the methodology described by Sinniger et al. (2013), Carreiro-Silva et al. (2017), Ocaña et al. (2017) and Ocaña and Çinar (2018). Nematocysts were examined with a light microscope equipped with a Nomarski differential interference contrast optic system. A minimum of ten polyps for each sample were examined. The classification and terminology of nematocysts followed Schmidt (1972) and further modifications by den Hartog (1980) and den Hartog et al. (1993). The terminology used by Ryland and Lancaster (2004) was also considered. Measurements of the cnidome are summarized in Table 2, where the ranges of length and width of nematocysts are included.

DNA extraction and sequence characterization

DNA was extracted from ethanol-preserved samples using a commercial kit *Quick-DNA Miniprep Plus* (Zymo Research). *COI* sequences were amplified following the Folmer et al. (1994) protocol, while ITS1, 5.8S, and ITS2 sequences were amplified as described in White et al. (1990) to be able to compare with the sequences already published on GenBank. PCR products were cloned using *pGEM-T Easy Vector* (Promega) in *Escherichia coli* JM109. Five clones for each sample and marker were selected to be sequenced by the Sanger method using a 3130 Genetic Analyzer (Applied Biosystems).

Mitochondrial genome sequencing, assembly, and annotation

The total DNA from the three morphotypes was sequenced using the NextSeq Illumina platform with paired-end 150 bp short reads (Macrogen, Korea). Mitochondrial genome was de novo constructed using the pipeline GetOrganelle using k-mer sizes of 21, 45, 65, 85, and 105, as proposed for animal mitogenomes by Jin et al. (2020).

The genomes obtained were annotated with Geneious Prime® v.2022.0.2 using the *Parazoanthus elongatus* McMurrich, 1904 mitochondrion complete genome sequence (Acc. Num.: NC_046405) as a reference source, with a 95% similarity and 65% cost matrix. Then, ORFs were searched using the "Find ORFs" tool, readjusting the gene length manually.

Sequence alignment and phylogeny

COI and ITS markers, belonging to other species from the Parazoanthidae family were retrieved from GenBank (Table S1). Analyses were performed at the family level as in Villamor et al. (2020), due to the considerable uncertainties in the current phylogeny and systematics of Parazoanthidae. Amplified COI sequences of the three analyzed species were aligned using MAFFT v.7.450 (Katoh and Standley. 2013) on Geneious Prime® v.2022.0.2, to search for diagnostic positions within the amplified fragments, following the results described in Sinniger et al. (2008).

For each marker, the sequences obtained from GenBank were aligned together with the amplified sequences using MAFFT v.7.450 on Geneious Prime® v.2022.0.2. Sequences were trimmed to remove primers, and jModelTest2 v.2.1.6 (Darriba et al. 2012) was run on the CIPRES portal (Miller et al. 2013) to identify the best nucleotide evolution model for each region. Maximum likelihood (ML) in PhyML v.3.3.2 0180621 and Bayesian interference (BI) in MrBayes v.3.2.6 trees were built using the best distance matrices model available on Geneious Prime® v.2022.0.2, based on the results of the jModelTest2 analysis. For *COI*, an analysis based on the parameters described in Sinniger et al. (2010) was also performed, with GTR nucleotide substitution matrix, a gamma 1 invariant model with six categories, estimated α-parameter and estimated frequencies of amino acids.

The alignment of mitochondrion concatenated genes was carried out using MUSCLE v.3.8.425 on Geneious Prime, following Poliseno et al. (2020). jModelTest2 v.2.1.6 (Darriba et al. 2012) was run on the CIPRES portal (Miller et al.

2013) on this alignment to identify the best nucleotide evolution model. Trees under maximum likelihood (ML) in PhyML v.3.3.20180621 and Bayesian interference (BI) in MrBayes v.3.2.6 were analyzed with Geneious Prime® v.2022.0.2.

Results

Ecology and in situ morphology observations

In this study, we found three different morphotypes of *Parazoanthus* living in the Alboran Sea. The species were classified based on the general morphological characteristics previously described (Pax 1937a and b, 1957; Herberts 1972; Gili et al. 1987; Ocaña et al. 2019).

P. axinellae sensu lato populations, or "morphotype 2," were found at all sampled locations, in a wide bathymetric range from 5 to at least 80 m. In Calahonda-Castell de Ferro SAC (Granada), it was observed growing in sympatry with *P. axinellae brevitentacularis*, sharing the same rocky walls. Although close to each other, the colonies are separate and clearly distinguishable (Fig. 1).

The presence of *P. axinellae brevitentacularis* was redetected in Ceuta, Spain (Ocaña et al. 2019), and detected for the first time in Granada, Spain, in Punta de la Mona (SAC) and Calahonda-Castell de Ferro SAC, mainly encrusting over rocky walls.

Another previously unclassified morphology, with smaller individuals than the previously described, was detected in all locations in Granada (Fig. 2). Colonies of this one were observed mainly incrusting walls and as a parasite of *Cliona* spp. and *Crambe crambe* sponges in Punta de la Mona SAC, Cerro Gordo Natural Reserve, and Calahonda-Castell SAC, living in a bathymetric range from 3 to 45 m. In the Calahonda-Castell de Ferro SAC, it was also observed living in sympatry with *P. axinellae* sensu lato on a rocky wall, but without mixing (Fig. 2a, b). Tentacle morphology was aberrant in the area where the colonies of the two morphologies of the population were in contact (Fig. 2c).

The ecological and morphological differences found in these two morphotypes with respect to *P. axinellae* sensu lato led us to their systematic evaluation for which macro and micromorphological (Systematics section) and genetic (Genetic results section) studies were carried out.

Systematics

Suborder Macrocnemina Haddon & Shackleton, 1891
Diagnosis: Zoantharians characterized by a complete fifth pair of mesenteries.
Family Parazoanthidae Delage & Hérouard, 1901
Genus *Parazoanthus* Haddon & Shackleton, 1891
Type species: *Palythoa axinella* Schimdt, 1862.
Diagnosis: Colonial zoantharians characterized by a mesogleal lacuna and by canals forming a "ring sinus" in the distal part of polyp. Fine mineral particles are incorporated in polyps.

***Parazoanthus brevitentacularis* Abel, 1959 stat. nov**

https://zoobank.org/259258C7-83BB-404B-8213-D3836F08785B

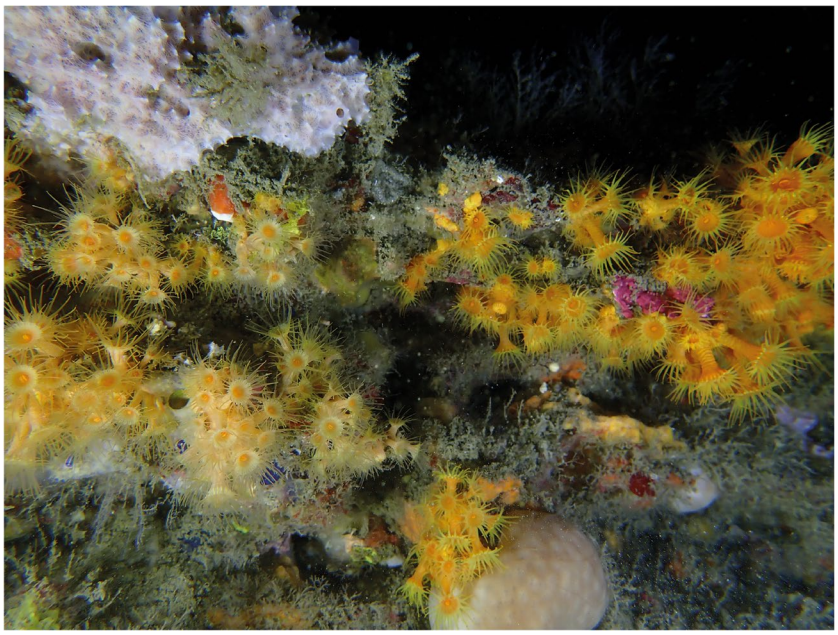

Fig. 1 Colonies of *P. axinellae* sensu lato (yellow, left) and *P. axinellae brevitentacularis* (orange, right) growing closely on rocky walls. Calahonda-Castell de Ferro SAC, Granada, Spain

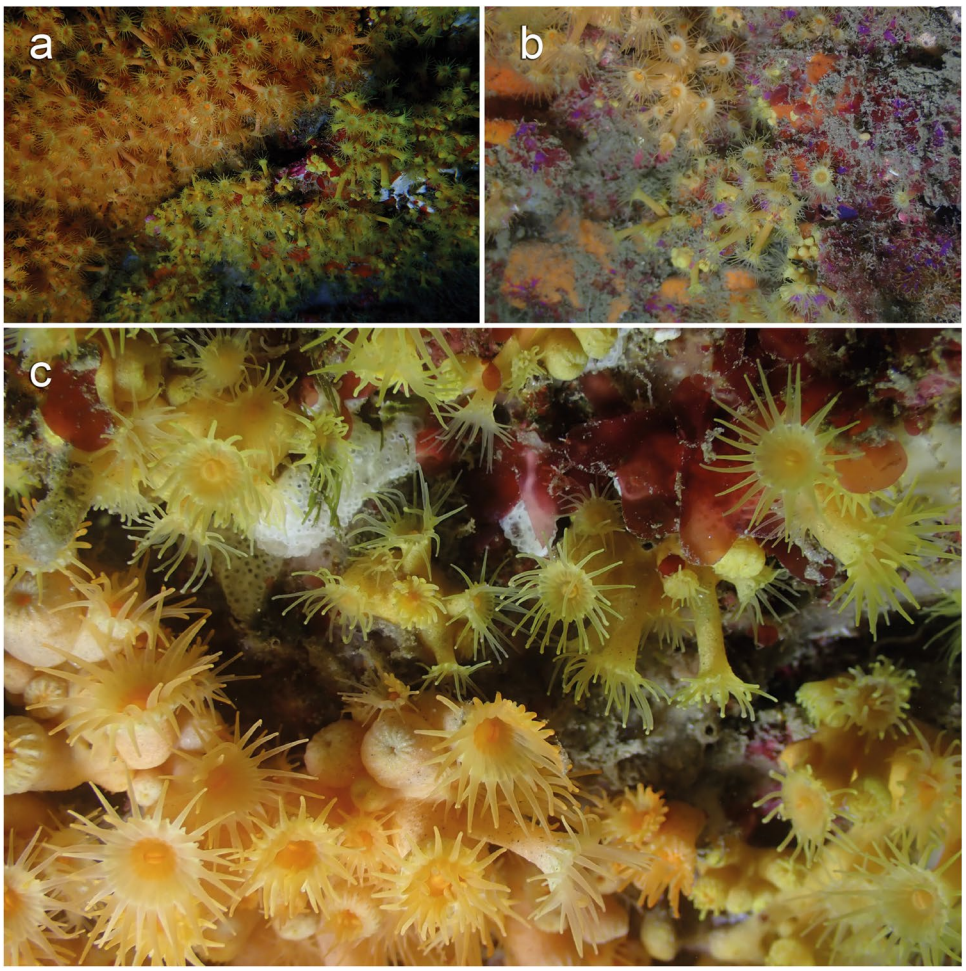

Fig. 2 **a**, **b** Colonies of *P. axinellae* (reddish yellow) and *P. franciscae* sp. nov. (greenish-yellow) growing closely together on rocky walls in Calahonda-Castell de Ferro SAC, Granada, Spain; **c** detail of tentacles showing different morphologies in the point of contact between colonies of two morphotypes of *Parazoanthus*

Previous names: *Parazoanthus axinellae brevitentacularis* Abel, 1959. (*P. axinellae* "stocky" and *P. axinellae* "morphotype 1").

Diagnosis Large colonies grouped in a common coenenchyma. Thick and encrusted polyps with very well-developed ectoderm, sand encrustation mainly under the ectoderm widespread in the outer mesoglea. The species is well distinguished by the single orange color in its entire body and the yellow or yellowish radial disc. Lacunae are concentrated in the inner mesoglea of the body wall. Large homotrich categories (P-mastigophores E) in tentacles and pharynx, a particular size of homotrich in the filaments, and two large homotrich categories (P-mastigophores E) of equal size in the body wall ectoderm.

Material examined

Neotype

A neotype has been proposed due to the lack of type material description in the original description.

SPAIN; 1 colony of 250 polyps growing on rocky cliffs; Spain, Granada, Gualchos-Castell de Ferro, Punta de Cerro Gordo; 36° 42′ 07″N 3° 24′ 35 ″W; 25–30 m depth; 21 Aug 2020; O. Ocaña and A. Rosales Ruiz leg; rocky slope and blocks with sandy bottom; MMC-T-65.

Paratypes

SPAIN; 1 colony of 35 polyps growing on rocky cliffs; Spain, Granada, Gualchos-Castell de Ferro, Punta de Cerro Gordo; 36° 42′ 07″N 3° 24′ 35″W; 25–30 m depth; 21 Aug 2020; O. Ocaña and A. Rosales leg; rocky slope and blocks with sandy bottom; MMC-T-66. SPAIN; 1 colony of 60 polyps growing on rocky cliffs; Spain, Granada, Gualchos-Castell de Ferro, Punta de Cerro Gordo; 36° 42′ 07″N 3° 24′ 35″W; 25–30 m depth; 21 Aug 2020; O. Ocaña and A. Rosales leg; rocky slope and blocks with sandy bottom; MMC-T-67. SPAIN; 1 colony of 60 polyps growing on rocky cliffs; Spain, Granada, Gualchos-Castell de Ferro, Punta de Cerro Gordo; 36° 42′ 07″N 3° 24′ 35″W; 25–30 m depth; 21 Aug 2020; O. Ocaña and A. Rosales leg; rocky slope and blocks with sandy bottom; MMC-T-68. SPAIN; 1 colony of 50–55 polyps growing on rocky cliffs; Spain, Granada, Gualchos-Castell de Ferro, Punta de Cerro

Gordo; 36° 42′ 07″N 3° 24′ 35″W; 25–30 m depth; 21 Aug 2020; O. Ocaña and A. Rosales leg; rocky slope and blocks with sandy bottom; MMC-T-69. SPAIN; 1 colony of 100 polyps growing on rocky cliffs; Spain, Granada, Gualchos-Castell de Ferro, Punta de Cerro Gordo; 36° 42′ 07″N 3° 24′ 35″W; 25–30 m depth; 21 Aug 2020; O. Ocaña and A. Rosales leg; rocky slope and blocks with sandy bottom; MMC-T-70.

Description

External anatomy

In living organisms, the body wall, capitulum, and oral disc are bright orange with thick opaque tentacles; the capitulum shows the distal radius of the first tentacle cycles of intense yellow or orange color. Mineral particles are present along the body wall, but they are conspicuous in retracted conditions. In preserved samples, polyps are 0.3–1 cm in height and a diameter of 0.2–0.5 cm, dark brown in color with no evidence of sand incrustations. All the polyps are embedded in a common tissue joined by a basal plate of coenenchyma; a connection among the colonies was not noticed. Four rows of 30–36 pointed tentacles, the last row is not complete at all; normally, the length of tentacles is shorter or equal to the expanded oral disc diameter; scapular ridges are strong and with a very conspicuous marginal tooth (Fig. 3a–d).

Internal anatomy

Mesenteries in a macrocnemic arrangement into four cycles of which the fourth is incomplete (36–40 mesenteries). Musculature well developed; retractor muscles are not present in mesenteries, but parietobasilar muscles are strong, with thick pennons; ectodermal musculature in tentacles visible forming insertions. Sphincter is strong, endodermal with 4–5 noticeable muscular sinus, short and concentrated in the upper part of the column; the pharynx is folded and presents a single long and prominent siphonoglyph. Thick mesoglea,

Fig. 3 **a–d** Macro photographs of *P. brevitentacularis* stat. nov. growing over a rocky substrate; **e**, **f** landscape photographs of *P. brevitentacularis* stat. nov. colonizing rocky walls in Calahonda-Castell de Ferro SAC, Granada

mineral particles concentrate in the outer mesoglea and are practically absent from ectoderm. Lacunae concentrate in the inner part of the mesoglea of the body wall. There was no indication of the presence of zooxanthellae (Fig. 4).

Cnidae

Measurements of the cnidome are summarized in Fig. 5 and Table 1. Common large homotrichs (P-mastigophores E), wide spirulae, and small homotrichs in tentacles. Common large typical spirulae in the pharynx. Presence of a particular category of large homotrichs (P-mastigophores E) in the filaments, and thick ovoid spirulae. Two categories of equal-size homotrichs (P-mastigophores E) and conspicuous special spirulae in the body wall. We did not observe any other categories of cnidome in the body wall.

Ecology and biological interactions

The species has been found growing mainly on bare rocky cliff or over calcareous algae at a depth ranging from 15 to 30 m (Fig. 3e, f). In the Ceuta region, *P. brevitentacularis* stat. nov. has been observed on the sponge *Petrosia ficiformis*.

Distribution

This species has been observed in Mediterranean and Macaronesia waters (Ocaña et al. 2019).

Parazoanthus franciscae Ocaña & Rosales Ruiz, 2023 sp. nov

https://zoobank.org/B6D22569-B57D-445F-AAC7-E476F8994EDA

Diagnosis Sand-encrusted ectoderm and mesoglea, forming tiny colonies of polyps with fine tentacles joined by a thin coenenchyme, small uniseriate groups. Also, colonies were assembled by a common rounded coenenchyma. Polyps are embedded in the common coenenchyma, easily distinguished by the presence of sand encrustation, yellowish

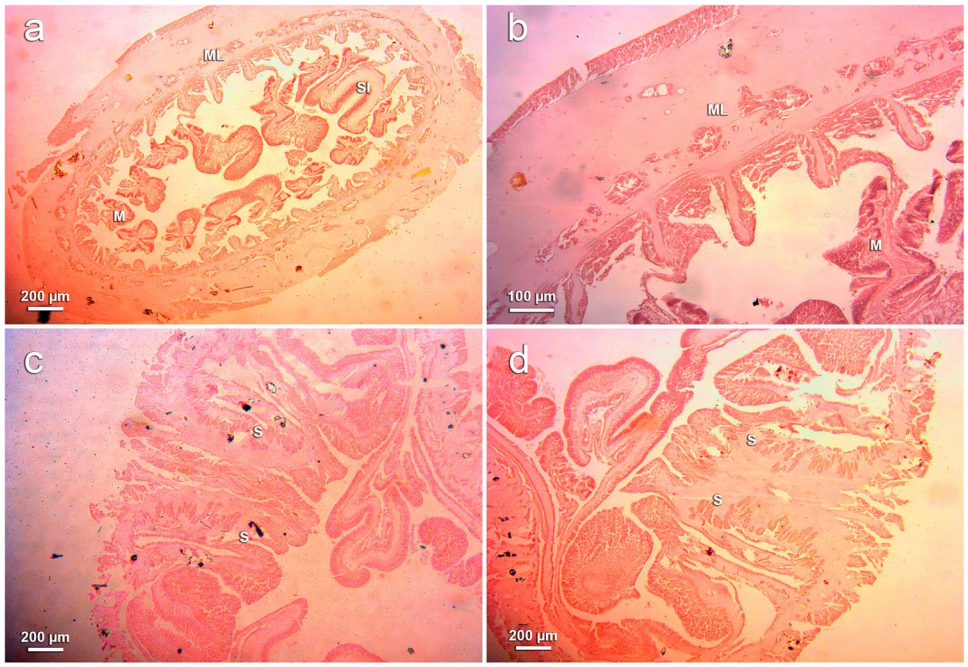

Fig. 4 **a** Transverse section of *P. brevitentacularis* stat. nov. showing the siphonoglyph (SI), mesenteries (M), and the ring mesogloeal lacunae (ML); **b** detail of mesogloeal lacunae (ML) and mesenteries (M); **c** longitudinal section showing the sphincter (S); **d** detail of the sphincter (S)

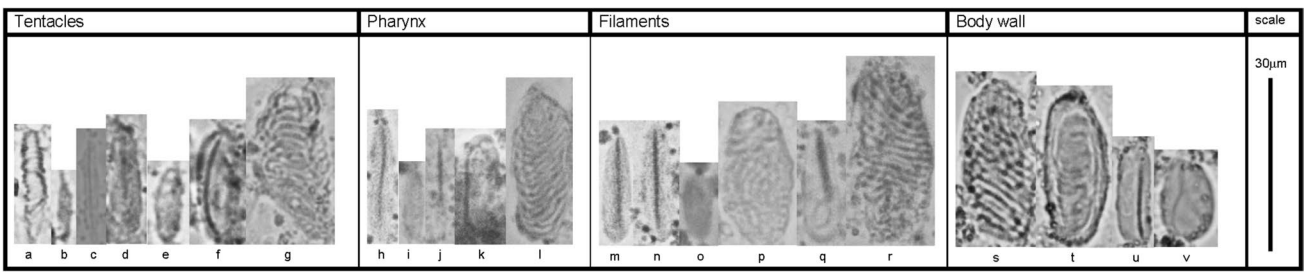

Fig. 5 Cnidome of *P. brevitentacularis* stat. nov. Cnidae in tentacles, pharynx, filaments, and body wall of *P. brevitentacularis* stat. nov

Table 1 Data resulting from the cnidome analysis of *P. brevitentacularis* stat. nov. Tissue where the different cnidae have been observed, nematocyst type, mean size, number, and frequency. The classification and terminology of nematocysts have been presented as established by Schmidt (1972), adapted by den Hartog (1980) and den Hartog et al. (1993), and include the terminology used by Ryland and Lancaster (2004)

Tissue	Nematocyst type	Mean and range of length and width of nematocyst capsules (μm)	Number	Frequency
Tentacles	Spirocysts (a)	(15–20) × (3–4)	20	vc
	Spirulae (b)	(8–9) × 2	5	uc
	Spirulae (c)	(15–17) × (2.5–3.5)	8	uc
	Spirulae (d)	(18–21) × (4–5)	20	c
	Homotrich (e)	(10–13) × (3–4)	10	rc
	Special spirulae (f)	(18–19) × (6–8)	6	uc
	Homotrich (g)	(21–31) × (10–16)	14	c
Pharynx	Spirulae (h)	(14–25) × (3–4)	15	c
	Homotrich (i)	(11–12) × (2–3.5)	5	uc
	Penicilli A (j)	18 × 3	1	r
	Special spirulae (k)	19 × 7	1	r
	Homotrich (l)	(25–32) × (10–14)	5	uc
Filaments	Spirulae (m)	(15–18) × (4–7)	10	rc
	Spirulae (n)	(18–19) × (4–5)	5	uc
	Homotrich (o)	(9–13) × (3.5–4)	2	r
	Homotrich (p)	(21–24) × (12)	6	rc
	Penicilli A (q)	(18–21) × (5–7)	15	rc-uc
	Homotrich (r)	34 × 13	1	r
Body wall	Homotrich (s)	(29–32) × (12–16)	30	vc
	Homotrich (t)	(26–31) × (10–12)	25	vc
	Special spirulae (u)	(16–21) × (6–8)	20	c
	Special spirulae (v)	(14–15) × (9)	2	r

color, and single-colored oral disc. Lacunae system is widespread in the mesoglea of the body wall. Cnidome with two categories of large and wide homotrichs (=holotrich or penicilli E in other nomenclatures). Elliptical special spirulae with a thick shaft (=homotrich, see Kise et al. 2018) in the body wall are detected also in other species (Carreiro-Silva et al. 2017; Ocaña and Brito 2004). There are also a variety of spirulae (=B-mastigophores or basitrichs) and a lesser number of penicilli (=P-mastigophores). Abundant special spirulae in tentacles and two large homotrich categories (P-mastigophores E) unequal in size in the body wall ectoderm. The species is mainly associated with other organisms (mainly sponges) as substrate.

Etymology The species is named *in memoriam* of Francisca Serrais Benavente, beloved wife of O. Ocaña, founder and first president of Fundación Museo del Mar de Ceuta (Spain).

Material examined

Holotype

SPAIN; 60 polyps divided in five small colonies growing on sponges; Spain, Granada, Gualchos-Castell de Ferro, Punta de Cerro Gordo; 36° 42′ 07″N 3° 24′ 35″W; 20–25 m depth; 20 Aug 2020; O. Ocaña and A. Rosales Ruiz leg; rocky slope and blocks with sandy bottom; MMC-T-58.

Paratypes

SPAIN; 15 small colonies growing on Cirripedia; Spain, Granada, Gualchos-Castell de Ferro, Punta de Cerro Gordo; 36° 42′ 07″N 3° 24′ 35″W; 20–25 m depth; 20 Aug 2020; O. Ocaña and A. Rosales Ruiz leg; rocky slope and blocks with sandy bottom; MMC-T-59. SPAIN; 16 colonies growing on stones, *Balanus* spp. and sponges; Spain, Granada, Almuñecar, Cueva de Cantarriján; 36° 43′ 47″N 3° 46′ 04″W; 3–5 m depth; 5 Aug 2021; O. Ocaña and A. Rosales Ruiz leg; rocky slope and blocks with sandy bottom; MMC-T-60. SPAIN; 10 colonies growing on stones, *Balanus* spp. and sponges; Spain, Granada, Almuñecar, Cueva de Cantarriján; 36° 43′ 47″N 3° 46′ 04″W; 3–5 m depth; 5 Aug 2021; O. Ocaña and A. Rosales Ruiz leg; rocky slope and blocks with sandy bottom; MMC-T-61. SPAIN; 14 colonies growing on stones, *Balanus* spp. and sponges; Spain, Granada, Almuñecar, Cueva de Cantarriján; 36° 43′ 47″N 3° 46′ 04″W; 3–5 m depth; 5 Aug 2021; O. Ocaña and A. Rosales Ruiz leg; rocky slope and blocks with sandy bottom; MMC-T-62. SPAIN; 20 colonies growing on stones, *Balanus* spp. and sponges; Spain, Granada, Almuñecar, Cueva de Cantarriján; 36° 43′ 47″N 3° 46′ 04″W; 3–5 m depth; 5 Aug 2021; O. Ocaña and A. Rosales Ruiz leg; rocky slope and blocks with sandy bottom; MMC-T-63. SPAIN; 20 colonies growing on stones, *Balanus* spp. and sponges; Spain, Granada, Almuñecar, Cueva de Cantarriján; 36° 43′ 47″N 3° 46′ 04″W; 3–5 m depth; 5 Aug 2021; O. Ocaña and A. Rosales Ruiz leg; rocky slope and blocks with sandy bottom; MMC-T-64.

Description

External anatomy

In living organisms, the body wall, capitulum, and oral disc are yellow to yellowish with thin translucent tentacles. Conspicuous mineral particles spread along the body wall. In preserved samples, polyps are 1–1.5 mm in diameter with a height of 1–2 mm, light brown to yellowish in color with abundant sand incrustations. Polyps forming small groups embedded and assembled in a common tissue and connected by a thin portion of coenenchyma, growing mainly over the sponges but also directly on rocky cliff. Three rows of 24–30 transparent pointed tentacles with parts of a fourth cycle can be observed in some specimens; normally, the length of tentacles is longer than the expanded oral disc diameter. Scapular ridges are generally inconspicuous, but marginal tooth can be easily distinguished in expanded polyps (Fig. 6a, b, and c).

Internal anatomy

Mesenteries in a macrocnemic arrangement into three cycles of which the third is incomplete (20 to 24 mesenteries were counted). Musculature is poorly developed; retractor muscles are not present in mesenteries; parietobasilar muscles are weak and inconspicuous along the mesenteries; ectodermal musculature in tentacles is visible forming short insertions. Sphincter is endodermal but short and concentrated in the upper part of the column; the pharynx is not folded and presents a single, non-prominent siphonoglyph. Widespread lacunae system in the mesoglea of the body wall. No evidence of the presence of zooxanthellae (Fig. 7).

Cnidae

Measurements of the cnidome are summarized in Fig. 8 and Table 2. Abundant special spirulae in tentacles together with tiny homotrichs and two fine spirulae categories; large spirulae and tiny homotrichs in the pharynx; two penicillie A categories and also small homotrichs in filaments; two large homotrichs (P-mastigophores E) unequal in size in the body wall ectoderm and special spirulae with a thick shaft in the body wall.

Ecology and biological interactions

Found growing on sponges (*Crambe crambe*, *Phorbas tenacior*, *Spirastrella cunctatrix*, and *Cliona viridis*) in shadow places, where it also can form colonies on *Balanus* spp., calcareous algae or even bare rocky reefs (Fig. 5d).

Distribution

The species have been observed principally in the Alboran sea inhabiting coastal caves and shaded places at a depth

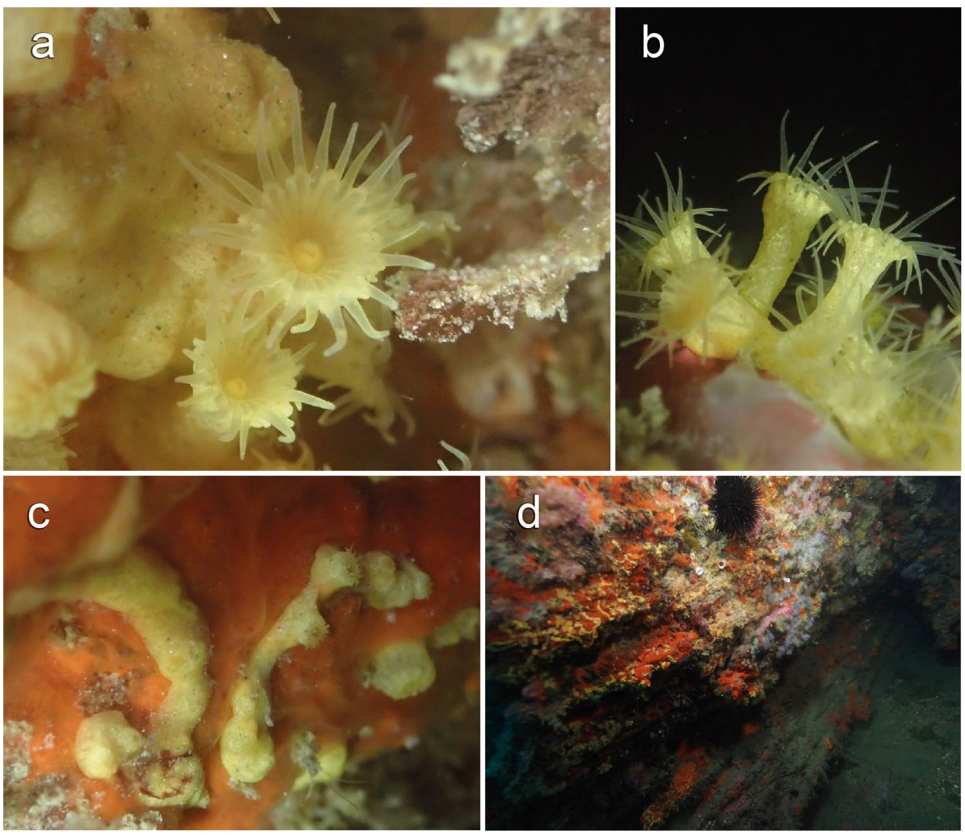

Fig. 6 **a**, **b**, **c** Macro photographs of *P. franciscae* sp. nov. growing over a rocky substrate; **d** landscape photographs of *P. franciscae* sp. nov. colonizing rocky walls in Calahonda-Castell de Ferro SAC, Granada

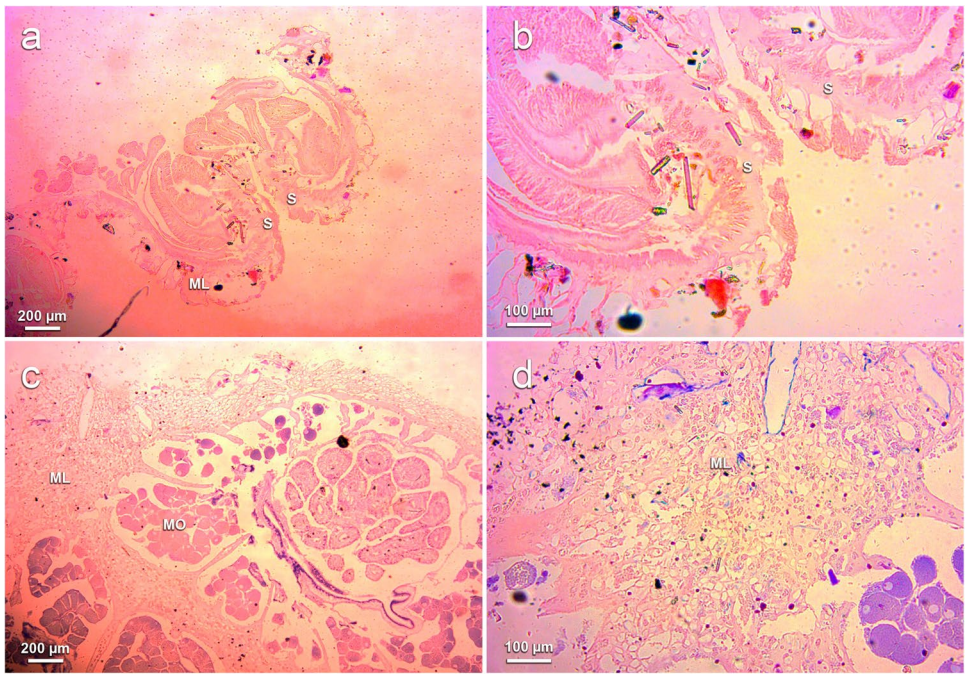

Fig. 7 **a** Longitudinal section of *P. franciscae* sp. nov. showing the sphincter (S) and general structure of the body wall with mesogloeal lacunae (ML); **b** detail of the sphincter (S); **c** longitudinal section showing mesenteries with ova (MO) and the mesogloeal structure with lacunae system (ML); **d** detail of the lacunae system (ML)

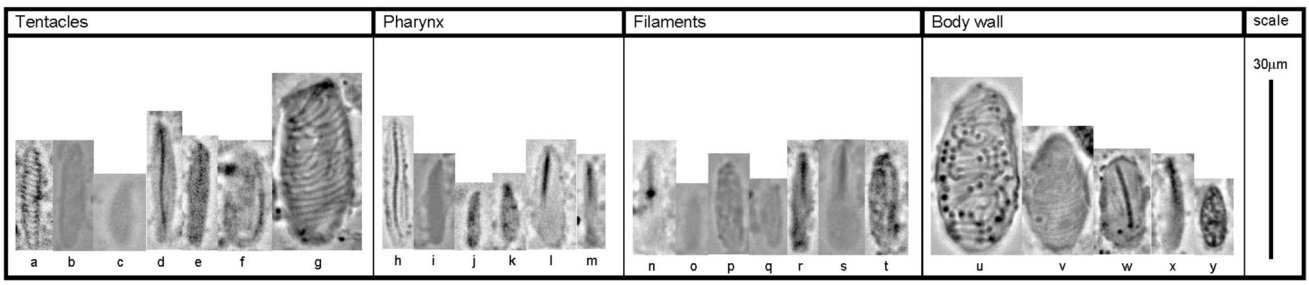

Fig. 8 Cnidome of *P. franciscae* sp. nov. cnidae in tentacles, pharynx, filaments, and body wall of *P. franciscae* sp. nov

of 3 to 45 m, with temperatures ranging from 13 to 21 °C. Colonies have also been observed in the Chafarinas Islands (Spain) (ETRS 89: 35° 11′ 07.1″N 2° 25′ 54.9″W) and Placer de las Bóvedas, Málaga (Spain) (ETRS 89: 36° 23′ 46.8″N 5° 00′ 17.9″W) in habitats with the same ecology.

Differential diagnosis

Differential diagnosis characters for *P. franciscae* sp. nov. and *P. brevitentacularis* stat. nov. have been summarized and compared with *P. axinellae* sensu lato (Table 3).

1. *P. franciscae* sp. nov.: Tiny to small size zoantharians with yellowish color on tentacles and disc, with orange disc; body wall with low to moderate quantity of incrusted particles, two categories of unequal sized homotrichs in the ectoderm of the body wall.
2. *P. brevitentacularis* stat. nov.: Large-size zoantharians with invariable orange color in column and disc; the latter also presents yellowish radiae and obvious thickening, especially evident along the second cycle of tentacles, body wall with low to moderate quantity of incrusted particles. Two large categories of equal-sized homotrichs in the ectoderm of the body wall.
3. *P. axinellae* sensu lato: Body wall totally covered by incrusted particles forming a thick layer. Small medium size zoantharians with yellowish color on tentacles and nearby disc portion close, with orange disc center and hypostome; one category of homotrichs in the ectoderm of the body wall.

In addition, an identification key has been included comparing the proposed species with the accepted subspecies of *P. axinellae* extracting the main diagnosis characters from Pax (1937a, b, and 1957), Abel (1959), Herberts (1972), Gili et al. (1987), and Ocaña et al. (2000) (Fig. 9).

Table 2 Data resulting from the cnidome analysis of *P. franciscae* sp. nov. Tissue where the different cnidae have been observed, nematocyst type, mean size, number, and frequency. The classification and terminology of nematocysts have been presented as established by Schmidt (1972), adapted by den Hartog (1980) and den Hartog et al. (1993), and include the terminology used by Ryland and Lancaster (2004)

Tissue	Nematocyst type	Mean and range of length and width of nematocyst capsules (μm)	Number	Frequency
Tentacles	Spirocysts (a)	(15–20)×(2–3)	20	vc
	Homotrich (b)	16×3.5	1	r
	Homotrich (c)	(10–11)×(2–3)	10	rc
	Spirulae (d)	(15–18)×(3–3.5)	20	c
	Spirulae (e)	(12–17)×(2–3.5)	15	rc
	Special spirulae (f)	(13–18)×(3.5–5)	25	vc
	Homotrich (g)	29×14	1	r
Pharynx	Spirulae (h)	(13–19)×(3–4)	20	c
	Spirulae (i)	(14–15)×(3)	5	uc
	Spirulae (j)	(8–9)×(2)	6	uc
	Homotrich (k)	(6–8)×(2–3)	10	rc
	Penicilli A (l)	15×5	1	r
	Penicilli A (m)	13×2	1	r
Filaments	Spirulae (n)	16×3	1	r
	Spirulae (o)	(6–8)×(1–1.5)	10	rc
	Homotrich (p)	15×3.5	1	r
	Homotrich (q)	(5–9)×(3)	5	rc
	Penicilli A (r)	(13–15)×(2–3)	15	c
	Penicilli A (s)	(12–15)×(4–5)	20	c
	Special spirulae (t)	(15×5)	1	r
Body wall	Homotrich (u)	(25–32)×(12–18)	20	c
	Homotrich (v)	(19–23)×(9–11)	20	c
	Special spirulae (w)	(13–19)×(7–9)	18	c
	Spirulae (x)	15×3	1	r
	Homotrich (y)	(11–12)×(4–5)	8	uc

Table 3 Main differences between the previously known *P. axinellae* subspecies, *P. brevitentacularis* stat. nov., and *P. franciscae* sp. nov

Subspecies	Color	Nº tentacles	Nº ridges	Nº septa	Spirocyst measurements	Homotrich ectoderm measurements
Parazoanthus axinellae adriaticus	Yellowish color in tentacles, orange disc center, and hypostome	26–30	14–16	28–32	10–16 μm	20–26 μm
Parazoanthus axinellae liguricus	Yellowish color in tentacles, orange disc center, and hypostome	36–38?	18?	36–38	15–17 μm	24–32 μm
Parazoanthus axinellae muelleri	Yellowish color in tentacles, orange disc center, and hypostome	26–36	14–18	28–36	16–21 μm	27–32 μm 26–34 μm
Parazoanthus franciscae sp. nov	Light brown to yellowish tentacles and oral disc	24–30	?, inconspicuous	20–24	15–20 μm	25–32 μm 19–23 μm
Parazoanthus brevitentacularis stat. nov	Orange color in column and disc; disc also with yellowish radiae and obvious thickening especially along the second cycle of tentacles	28–32	14–16	34–38	20–21 μm	29–32 μm 26–31 μm

Genetic results

Complete mitochondrial genomes

A total of 36,917,848 sequences were obtained from the Illumina sequencing of *P. brevitentacularis* stat. nov., 38,257,504 from *P. axinellae* and 38,868,432 from *P. franciscae* sp. nov.

Three mitochondrion genome consensus sequences were assembled and annotated with a size of 20,979 bp for *P. axinellae* sensu lato; 21,184 bp for *P. brevitentacularis* stat. nov.; and 21,135 bp for *P. franciscae* sp. nov. (Table S5). All three genomes retain the same number (17) and architecture of genes (Fig. S1). Out of the 17 genes annotated, COI was significantly important due to the presence, within

Identification key

1 Body wall totally covered by incrusted particles forming a thick layer.....2
Body wall with low to moderate quantity of incrusted particles, never forming a thick layer 3
2 Small medium size zoanthids with yellowish colour on tentacles and nearby disc portion close, orange disc center and hypostome. Polyps with 26-30 tentacles; 14-16 ridges; 28-32 septa and one category of homotrichs in the ectoderm of the bodywal.....***Parazoanthus axinellae adriaticus***
Small medium size zoanthids with yellowish colour on tentacles and nearby disc portion close, orange disc center and hypostome Polyps with 36-38 tentacles: 28 ridges; 36-38 septa and one category of homotrichs in the ectoderm of the body wall.....***Parazoanthus axinellae liguricus***
Small medium size zoanthids with yellowish colour on tentacles and nearby disc portion close, orange disc center and hypostome Polyps with 26-36 tentacles: 14-18 ridges; 28-36 septa and two categories of equal sized homotrichs in the ectoderm of the body wall.....***Parazoanthus axinellae muelleri***
3 Tiny to small size zoanthids with yellowish colour on tentacles and disc, with orange disc; two categories of inequal sized homotrichs in the ectoderm of the body wall.....***Parazoanthus franciscae* sp. nov.**
Large size zoanthids with invariable orange colour in column and disc; the latter also presents yellowish radiae and obvious thickening, especially evident along the second cycle of tentacle.....***Parazoanthus brevitentacularis* stat. nov.**

Fig. 9 Identification key showing the main differences between the known Mediterranean species and subspecies of the genus *Parazoanthus*

its intron, of a homing endonuclease gene (*HEG*), which were also detected in anemones (Beagley et al. 1996) and other zoantharians (Sinniger et al. 2007; Chi and Johansen 2017). Also, COI was the only reversed gene detected in the genome. This has been previously reported in some zoantharian species (Chi and Johansen 2017). The sequences of these three genomes were aligned with five other sequences belonging to other species of the order Zoantharia obtained from GenBank (Table S5). The three orders were congruent with the one described by Poliseno et al. (2020). Genes and intergenic regions of each genome were analyzed separately.

The genetic distance table (Table S6) based on concatenated genes shows a low interspecific variability within the *Parazoanthus* genus, ranging from 0.001 between *P. franciscae* sp. nov. and *P. axinellae* sensu lato, and between *P. brevitentacularis* stat. nov. and *P. elongatus*, to 0.007 between *P. elongatus* and *P. swiftii*. The same distance ranges between species were evident when concatenated intergenic regions were analyzed (Table S7), showing a stronger relationship between *P. franciscae* sp. nov. and *P. axinellae* sensu lato (0.007) and between *P. brevitentacularis* stat. nov. and *P. elongatus* (0.005). Phylogenetic trees, using gene and intergenic region information, constructed using both Bayesian (Fig. S5) and maximum likelihood approaches (Fig. 10) were congruent. *Savalia savaglia* is placed in a basal position to the clade containing the *Parazoanthus* species (ML, 100%; BI, 1.0), with *Parazoanthus swiftii* being at the base of the rest of the *Parazoanthus* genus (ML, 100%; BI, 1.0). ML and BI analyses showed the presence of two clades within *Parazoanthus* (ML, 77.9%; BI, 1.0). One is composed of *Parazoanthus elongatus* and *P. brevitentacularis* stat. nov., with a ML 100% support and BI 1.0. The other is composed of *P. axinellae* sensu lato and *P. franciscae* sp. nov., being independent with a ML 100% support and 1.0 BI.

PCR amplification of markers

Mitogenome analyses were complemented by the analysis of mitochondrial and ribosomal molecular marker regions. For the COI region, 23 sequences were amplified from samples of *P. axinellae* sensu lato, *P. brevitentacularis* stat. nov., and *P. franciscae* sp. nov. (Table S1) and aligned with a total of 98 GenBank COI sequences from 11 species of the Parazoanthidae family (Table S1). The genetic distances (Table S2)

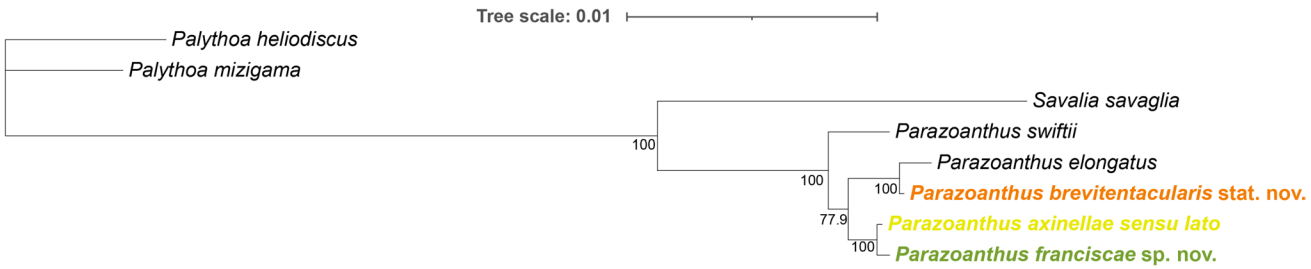

Fig. 10 Maximum likelihood phylogenetic tree of staggered gene coding regions. TVM + I + G was identified on the jModelTest2 ratio test as the best-fitting nucleotide substitution model for the alignments, with GTR + I + G being the best-fitting model available in Geneious Prime for Bayesian and maximum likelihood analyses. Tree edited on iTOL (Letunic and Bork 2021)

showed very low intra- and interspecific values between *P. axinellae* sensu lato, *P. brevitentacularis* stat. nov., *P. franciscae* sp. nov., and the other species of the genus, ranging from 0 to 0.014. The sequences did not cluster according to their taxonomic origin. This resulted in unresolved phylogenetic trees, unable to differentiate species, neither with the Bayesian method (Fig. S3) nor with the maximum likelihood method (Fig. S4). The alignment of the amplified COI sequences was examined to detect molecular signatures for species diagnosis showing results, while a high value of intraspecific variation was detected specially in *P. franciscae* sp. nov. The positions 143, 252, and 320 of the amplified fragments show diagnostic position for *P. brevitentacularis* stat. nov. against *P. axinellae* and *P. franciscae* sp. nov. Position on 143 of *P. brevitentacularis* stat. nov. is an adenine, while in the others is a guanine (Fig. S5). About 252 and 320 positions, in *P. brevitentacularis* stat. nov., are thymines, while cytosines in the others (Figs. S6 and S7). Also, position 532 seems to be different in *P. brevitentacularis* stat. nov., with a cytosine when compared to *P. axinellae* sequences, with a thymine. Nevertheless, on one of the sequences of *P. franciscae* sp. nov. (OQ456489), this position is also a cytosine, while in the other sequences of the species is a thymine (Fig. S8).

For the ribosomal region (ITS1-5.8S-ITS2), 25 amplified sequences from *P. axinellae* sensu lato, *P. brevitentacularis* stat. nov., *P. franciscae* sp. nov., and, additionally, *S. savaglia*, were analyzed together with 95 sequences from 11 species belonging to the Parazoanthidae and Epizoanthidae families, the latter as the outgroup (Table S3). For the analyses, the ITS sequences were concatenated. The distances showed a 30-fold higher variation range between species (Table S4) than the one observed in the COI sequences. Thus, the genetic distances showed a low intraspecific variability for all the species analyzed, ranging from 0 (*P. juanfernandezii*, only one sequence available) or 0.002 (*P. elongatus* and *P. anguicomus*, with only two sequences available) to 0.01 in *P. franciscae* sp. nov. The interspecific distances of the two species described in this work were higher in some cases than those between previously accepted species. Thus, *P. brevitentacularis* stat. nov. showed a higher interspecific distance value with *P. axinellae* sensu lato (0.239) than *P. axinellae* sensu lato with close species such as *P. anguicomus* (0.117) or *P. atlanticus* (0.205). Similarly, the new species *P. franciscae* sp. nov. showed a higher genetic distance with *P. axinellae* sensu lato (0.148) than the one shown between *P. axinellae* sensu lato and *P. anguicomus* (0.117) and about fourfold higher than the one between *P. darwinii* and *P. swiftii* (0.038).

Phylogenetic trees derived from Bayesian (Fig. 11) and maximum likelihood (Fig. S9) analyses were congruent, clustering the species independently and showing the same topography observed when performing the mitogenome analysis. Sequences from *P. brevitentacularis* stat. nov. grouped independently from *P. axinellae* sensu lato (ML 70.4%; BI, 1.0), with most of the *P. axinellae* "stocky" sequences from the Mediterranean obtained in Villamor et al. (2020) retrieved from GenBank. It was named as the *P. brevitentacularis* cluster, being closely related to *P. elongatus* and *P. juanfernandezii* from the Pacific Ocean (ML, 73.5%; BI, 0.88) (Fig. 11). Nine sequences of *P. axinellae* "stocky" morphotype from Villamor et al. (2020) clustered in an independent sibling clade with a high bootstrap (ML, 99.2%) and Bayesian posterior probability (BI, 1.0) support, named as "stocky-2" cluster (Fig. 11). *P. franciscae* sp. nov. sequences appear as a close but independent cluster to the specimens in the *P. axinellae* sensu lato clade (ML, 92.3%; BI, 1.0) and close to *P. anguicomus* from the Northeast Atlantic, with medium ML bootstrap and high Bayesian probability values (ML, 48.2%; BI, 0.8). *P. atlanticus* is found in a more distant and basal position from those clades. *P. axinellae* "slender" sequences from the Mediterranean retrieved from GenBank grouped with those of *P. axinellae* sensu lato amplified in this study. Only one sequence, the *P. axinellae* "slender" (MT771127.1) derived from the Villamor et al. (2020) study was observed outside this group with high support (ML, 98.5%; BI, 1.0).

Discussion

In this research, the divergence observed at morphological, ecological, histological, and genetic levels within the *P. axinellae* complex has led to the reclassification of *P. axinellae brevitentacularis* as *P. brevitentacularis* stat. nov. and the description of the new species *P. franciscae* sp. nov. in the Alboran Sea.

The morphological data described establishes diagnostic characters based on micromorphology, macromorphology, and histology, supporting previously published data (Abel 1959; Gili et al. 1987; Ocaña et al. 2019). These results have been summarized in a taxonomical key (Table 3). The cnidome was deeply studied for the first time in the two species proposed in this work (Figs. 5 and 8, Tables 1 and 2).

When compared with the previously known *P. axinellae* subspecies, *P. franciscae* sp. nov. showed clear divergences. According to Herberts (1972) and Gili et al. (1987), there are several subspecies or varieties within *P. axinellae* (Fig. 11). First, the oral disc shares the same color as the rest of the polyp, while in the *P. axinellae* subspecies, the oral disc is orange. The number of tentacles is also lower (24–30) but overlaps with *P. axinellae adriaticus* (26–30). The ridges are inconspicuous in *P. franciscae* sp. nov., while present in high numbers in the *P. axinellae* subspecies. There is also a small number of septa in *P. franciscae* sp. nov. (20–24), not overlapping with any subspecies. On the other hand, while the spirocyst measurements may overlap in size between *P. franciscae* sp. nov. and the subspecies, the presence of special size homotrich is a determinant factor.

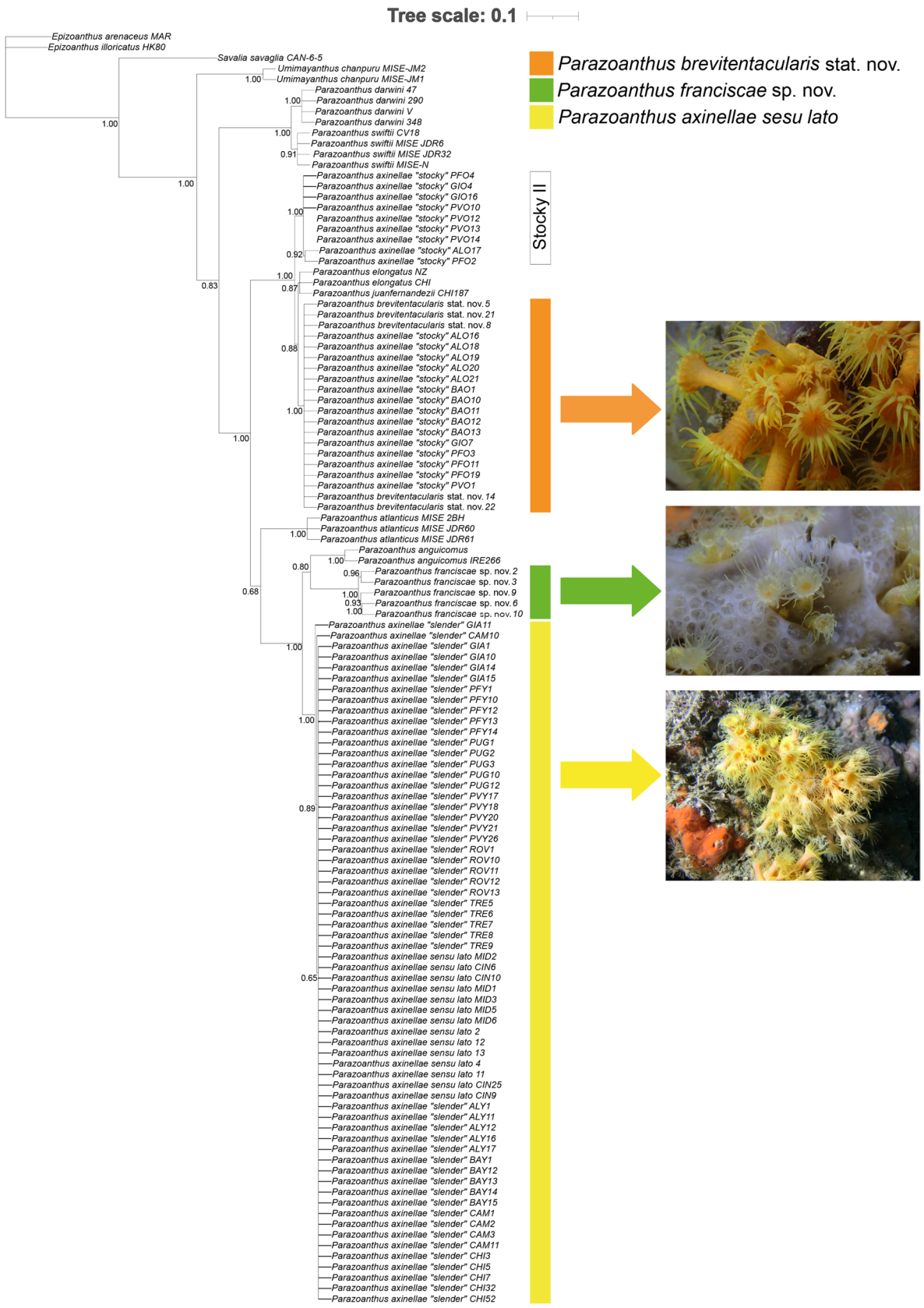

Fig. 11 Bayesian phylogenetic tree of *ITS* regions using HKY + G as substitution model. Tree edited in iTOL (Letunic and Bork 2021) and Adobe Illustrator 25.4.1

The ecological differences observed between *P. axinellae* sensu lato, *P. brevitentacularis* stat. nov., and *P. franciscae* sp. nov. are also remarkable. *P. axinellae* sensu lato has been found living in a wide bathymetric range, between the first meters of infralittoral environments to at least 80 m, encrusting large portions of rocky walls or parasitizing *Axinella* spp. sponges, commonly related to scyaphyllic areas. *P. brevitentacularis* stat. nov. is distributed in a narrower bathymetric range, being found from 15 to almost 30 m, mainly encrusting rocky walls, where it can cover areas larger than 3–4 m^2, or over coralline algae, and in more rheophilic habitats than the others. *P. franciscae* sp. nov. has been found living at depths ranging from 3 to 45 m, with most of the colonies being detected between 15 and 35 m, mainly as a parasite of sponges (*C. crambe*, *P. tenacior*, *S. cunctatrix*, and *C. viridis*) in shaded areas, where it also can form colonies on *Balanus* spp., calcareous algae or even bare rocky reefs.

One of the hypotheses that may explain the great diversity of zoanthid morphotypes is based on their morphological plasticity (Reimer et al. 2006; Costa et al. 2011). In *Parazoanthus*, this has been used to explain the differences between morphotypes, as there are no records of different morphotypes growing closely together. However, in our study, we found the morphologies currently associated with *P. brevitentacularis* stat. nov. and *P. franciscae* sp. nov. growing in sympatry with *P. axinellae* sensu lato, sharing the same rocky walls (Figs. 1 and 2). The colonies did not merge with each other, and no signs of hybridization were found, but in the areas where different species made contact, the tentacles showed morphological aberrations (Fig. 2) that might be related with repulsion or attack mechanisms.

In recent years, the use of whole mitochondrial genome sequences has been proposed as an effective tool for phylogenetic studies, particularly in groups where single-gene markers such as COI or cytochrome b (CYTB) fail to resolve species relationships (Poliseno et al. 2020; Barrett et al. 2020), as observed in our case (Table S2). Nevertheless, some diagnostic positions were found in *P. brevitentacularis* stat. nov. amplified COI sequences, while a high value of intraspecific variation was also detected (Figs. S7 and S8) which might be related with low-resolution sequencing or, based on Sinniger et al. 2008, with the existence of cryptic species within the samples.

In this study, we characterized the complete mitochondrial genome of the three taxa involved. The analysis of gene coding and intergenic concatenated regions showed divergence between species, although the distances between them were moderate due to the low rate of change of the mitogenome within this group (Tables S6 and S7). However, the genetic distances observed in both gene and intergenic regions of the mitogenome between *P. brevitentacularis* stat. nov. and *P. axinellae* sensu lato were always equivalent or greater than those found between *P. brevitentacularis* stat. nov. and an already accepted species such as *P. elongatus*. Both species have divergent morphological characters and inhabit spatially and ecologically quite distant ecosystems, which makes it difficult to regard them as the same species. This result would support the contention that *P. brevitentacularis* stat. nov. is a different species, separated from *P. axinellae* sensu lato and *P. elongatus*. In this sense, it is shown here that the distances between *P. franciscae* sp. nov. and *P. axinellae* sensu lato were always equivalent (0.001 in genes) or greater (0.007 in intergenic regions) than those found between *P. brevitentacularis* stat. nov. and *P. elongatus* (0.001 and 0.005, respectively), which would indicate a level of genetic differentiation within the range observed between species in this group.

The hypothesis presented, based on morphology and mitochondrial DNA, is also supported by ribosomal internal transcribed spacer (*ITS1* and *ITS2*) sequences. The distance analysis showed values of intraspecific variability and interspecific divergence of the species *P. brevitentacularis* stat. nov., *P. axinellae* sensu lato, and *P. franciscae* sp. nov. that were very similar to those obtained in other species of the genus (Table S4). The phylogenetic tree obtained from these distances reveals the separation of *P. brevitentacularis* stat. nov. and *P. franciscae* sp. nov. from the *P. axinellae* sensu lato complex, constituting independent taxa. These results are concordant with the results of the comparation.

In the case of *P. brevitentacularis* stat. nov., our analysis positions it as a widely divergent taxon from *P. axinellae* sensu lato and mixing ITS sequences in the phylogenetic tree with *P. axinellae* "stocky" sequences. This clade is closely related to Atlantic and Pacific species, such as *P. elongatus* (similar result to that obtained with the mitogenome DNA, Fig. 10), *P. juanfernandezii* or distantly, with *P. atlanticus* than with *P. axinellae* sensu lato. However, several sequences from *P. axinellae* "stocky" obtained by Villamor et al. (2020), clustered outside of the *P. brevitentacularis* stat. nov. group. The presence of this separate cluster (named stocky 2, Fig. 11) can be related with the existence of a cryptic species, as the clades seem to be sympatric in some of the areas sampled by these authors. Although for the nomenclature revision, we have assumed the simplest explanation following the principle of parsimony, understanding *P. brevitentacularis* stat. nov. as a species extended along the whole Mediterranean; this is an interesting point for further research, and if the assumption of the cryptic species is true, the real identity of the type population described by Abel (1959) should be clarified.

With respect to *P. franciscae* sp. nov., this is the first description and characterization of the species using genetic and morphological analyses. The phylogenetic analysis (Fig. 11, Fig. S7, and Table S4) showed a closer relationship with *P. anguicomus* than with *P. axinellae* sensu lato, the latter

being closer than *P. brevitentacularis* stat. nov. (similar result to that obtained with the mitogenomic DNA, Fig. 10). The species showed a restricted distribution, being found only in small colonies in enclosed areas of the Alboran Sea, making it sensitive to disturbances in the areas where it is present. An intensive re-evaluation of zoanthid species is needed, as there may be more undescribed taxa at risk of species loss.

Our results demonstrate that an integrative method, combining in situ ecological observations, macro- and micromorphology, and molecular genetics techniques, works synergistically to enhance understanding of the biodiversity within an area, revealing cryptic species that may be concealed within currently recognized taxa. Indeed, this approach has successfully resolved taxonomic uncertainties within an important group in the Alboran Sea and Mediterranean ecosystems.

Supplementary Information The online version contains supplementary material available at https://doi.org/10.1007/s12526-024-01493-x.

Acknowledgements This study was made possible thanks to the disinterested financial support of Fundación Biodiversidad, the Spanish Ministry for Ecological Transition and Demographic Challenge, and the CEI·MAR Foundation and Gestión Técnica Medioambiental Sur S.L.U. The authors are also grateful to Guillermo Chill, for his collaboration to this work as a master's student. To Manuel García Díaz, the rest of the fellow colleagues from the Fundacion Museo del Mar de Ceuta, and Silke Martínez Moreno, from the University of Granada, for their participation in the sampling process throughout the different campaigns around the Alboran Sea, and to Dacio Correa Betancourt for his collaboration during the sample analysis process. We also want to thank Aula del Mar CEI·MAR at the University of Granada, for helping us in the sampling process and the maintenance of living organisms, the Spanish National Parks Autonomous Organism, which support was key to develop the studies in the Chafarine Islands Archipelago, and the Spanish Ministry of Defense, to the Army, and especially the Guardia Civil Marine Service, for helping and ensuring the good development of the research performed on these islands. Fundación Museo del Mar de Ceuta wants to especially thank the Ceuta Port Authority for providing the space where the office and the laboratories of the entity are located. This support was key for the research performed in this work.

The authors would like to contribute these species to the Ocean Census Programme (https://oceancensus.org/), being Ocean Census Species number 32 *Parazoanthus franciscae* sp. nov. and number 33 *Parazoanthus brevitentacularis* stat. nov.

The authors wish to express their gratitude to the reviewers, the editor, and the editorial office for their constructive contributions and feedback during the manuscript revision process.

Funding Funding for open access publishing: Universidad de Granada/CBUA. This study was performed within the framework of the MESO_Alboran 2 project, developed with the collaboration of the Biodiversity Foundation of the Ministry for Ecological Transition and the Demographic Challenge, through the Pleamar Programme, and is co-financed by the European Union through the European Maritime, Fisheries and Aquaculture Fund, MESO_Alboran project, in collaboration with Biodiversity Foundation, the Spanish Ministry for Ecological Transition and Demographic Challenge, through the Pleamar Program, co-financed by the European Union Maritime and Fisheries Fund. The study was also supported by the Spanish Ministry for Ecological Transition and Demographic Challenge, through the project "Morphotaxonomic, ecological and genetic study of the Parazoanthidae family in the Atlanto-Mediterranean context: Bases to understand and conserve the different species with relevant ecologies" and the CEI·MAR Foundation and Gestión Técnica Medioambiental Sur S.L.U, which co-founded the project "Development of molecular markers in anthozoans from the Alboran Sea for biodiversity, environmental and biotechnological studies".

Declarations

Conflict of interest The authors declare no competing interests.

Ethical approval The authors declare they have followed all applicable international and national guidelines for sampling, care, and experimental use of organisms for this study, and all necessary approvals have been obtained. Samples were collected under the Resolution of the Territorial Delegate for Sustainable Development of the Junta de Andalucía in Granada authorizing sampling along the coast of Granada provided by Junta de Andalucía and the permission SGBTM/BDM/AUTSPP/28/2022 provided by the general sub-direction of terrestrial and marine biodiversity of the Spanish Ministry of Ecological Transition and the Demographical Challenge, following the procedures exposed on these resolutions. Documentary evidence is available on request.

Sampling and field studies All necessary permits for sampling and observational field studies have been obtained by the authors from the competent authorities and are mentioned in the acknowledgements, if applicable. The study is compliant with CBD and Nagoya protocols.

Data availability The datasets generated during the current study are available in the NCBI GenBank repository. Samples are available to re-analyses on the collection of the Museo del Mar de Ceuta on a reasonable request.

Author contributions Alfredo Rosales Ruiz, Oscar Ocaña, Roberto de la Herrán, Carmelo Ruiz Rejón, and Francisca Robles conceived and designed this research. Samples were collected by Alfredo Rosales Ruiz, Oscar Ocaña, and Ander Congil Ross. Oscar Ocaña conducted the morphological studies. Genetic lab works were performed by Alfredo Rosales Ruiz, Roberto de la Herrán, and Francisca Robles, being the results analyzed also by Rafael Navajas-Pérez and Carmelo Ruiz Rejón. Alfredo Rosales Ruiz and Oscar Ocaña wrote the manuscript. All authors read and approved the manuscript.

References

Abel EF (1959) Zur Kenntnis der marinen Höhlenfauna unter besonderer Berücksichtigung der Anthozoen. Pubblicazioni della Stazione Zoologica di Napoli 30:1–94

Barrett NJ, Hogan RI, Allcock AL, Molodtsova T, Hopkins K, Wheeler AJ, Yesson C (2020) Phylogenetics and mitogenome organisation

in black corals (Anthozoa: Hexacorallia: Antipatharia): an order-wide survey inferred from complete mitochondrial genomes. Front Mar Sci 7:440

Beagley CT, Okada NA, Wolstenholme DR (1996) Two mitochondrial group I introns in a metazoan, the sea anemone Metridium senile: one intron contains genes for subunits 1 and 3 of NADH dehydrogenase. Proc Natl Acad Sci 93(11):5619–5623

Cachet N, Genta-Jouve G, Ivanisevic J, Chevaldonné P, Sinniger F, Culioli G, Thomas OP (2015) Metabolomic profiling reveals deep chemical divergence between two morphotypes of the zoanthid Parazoanthus axinellae. Sci Rep 5(1):8282

Carreiro-Silva M, Ocaña O, Stanković D, Sampaio Í, Porteiro FM, Fabri MC, Stefanni S (2017) Zoantharians (Hexacorallia: Zoantharia) associated with cold-water corals in the Azores region: new species and associations in the deep sea. Front Mar Sci 4:88

Chen IP, Tang CY, Chiou CY, Hsu JH, Wei NV, Wallace CC, Meir P, Wu H, Chen CA (2009) Comparative analyses of coding and noncoding DNA regions indicate that Acropora (Anthozoa: Scleractina) possesses a similar evolutionary tempo of nuclear vs. mitochondrial genomes as in plants. Mar Biotechnol 11(1):141–152

Chi SI, Johansen SD (2017) Zoantharian mitochondrial genomes contain unique complex group I introns and highly conserved intergenic regions. Gene 628:24–31

Concepcion GT, Medina M, Toonen RJ (2006) Noncoding mitochondrial loci for corals. Mol Ecol Notes 6(4):1208–1211

Costa DL, Gomes PB, Santos AM, Valença NS, Vieira NA, Pérez CD (2011) Morphological plasticity in the reef zoanthid Palythoa caribaeorum as an adaptive strategy. Ann Zool Fenn 48(6):349–358

Darriba D, Taboada GL, Doallo R, Posada D (2012) jModelTest 2: more models, new heuristics and parallel computing. Nat Methods 9(8):772–772

Delage Y, Hérouard E (1901) Traité de zoologie concrète. Tome II – Deuxième partie. Les coelentérés. Schleicher Frères, Paris, 848 pp

Den Hartog JC (1980) Caribbean Shallow Water Corallimorpharia. Zool Verh 176(1):1–83

Den Hartog JC, Ocaña O, Brito A (1993) Corallimorpharia collected during the CANCAP expeditions (1976–1986) in the south-eastern part of the North Atlantic. Zool Verh 282(1):1–76

Dohna TA, Kochzius M (2016) Obstacles to molecular species identification in sea anemones (Hexacorallia: Actiniaria) with COI, a COI intron, and ITS II. Mar Biodivers 46(1):291–297

Folmer O, Black M, Hoeh W, Lutz R, Vrijenhoek R (1994) DNA primers for amplification of mitochondrial cytochrome c oxidase subunit I from diverse metazoan invertebrates. Mol Mar Biol Biotech 3(5):294–299

France SC, Hoover LL (2002) DNA sequences of the mitochondrial COI gene have low levels of divergence among deep-sea octocorals (Cnidaria: Anthozoa). Hydrobiologia 471:149–155

Fujii T, Reimer J (2013) A new family of diminutive zooxanthellate zoanthids (Hexacorallia: Zoantharia). Zool J Linn Soc 169(3):509–522

Fujii T, Reimer JD (2011) Phylogeny of the highly divergent zoanthid family Microzoanthidae (Anthozoa, Hexacorallia) from the Pacific. Zoolog Scr 40(4):418–431

Fukami H, Knowlton N (2005) Analysis of complete mitochondrial DNA sequences of three members of the *Montastraea annularis* coral species complex (Cnidaria, Anthozoa, Scleractinia). Coral Reefs 24:410–417

Gili JM, Pages F, Barangé M (1987) Zoantarios (Cnidaria, Anthozoa) de la costa y de la plataforma continental catalanas (Mediterráneo occidental). Miscel· lània Zoològica, pp 13–24

Haddon AC, Shackleton AM (1891) A revision of the British actiniæ. Part II.: The Zoantheæ. Sci Trans R Dublin Soc 4(12):609–672

Hebert PD, Cywinska A, Ball SL, DeWaard JR (2003) Biological identifications through DNA barcodes. Proc R Soc Lond Ser B: Biol Sci 270(1512):313–321

Hellberg ME (2006) No variation and low synonymous substitution rates in coral mtDNA despite high nuclear variation. BMC Evol Biol 6:1–8

Herberts C (1972) Contribution à l'étude écologique de quelques zoanthaires tempérés et tropicaux. Mar Biol 13:127–136

Huang D, Meier R, Todd PA, Chou LM (2008) Slow mitochondrial COI sequence evolution at the base of the metazoan tree and its implications for DNA barcoding. J Mol Evol 66:167–174

Jin JJ, Yu WB, Yang JB, Song Y, DePamphilis CW, Yi TS, Li DZ (2020) GetOrganelle: a fast and versatile toolkit for accurate de novo assembly of organelle genomes. Genome Biol 21:1–31

Katoh K, Standley DM (2013) MAFFT multiple sequence alignment software version 7: improvements in performance and usability. Mol Biol Evol 30(4):772–780

Kise H, Dewa N, Reimer JD (2018) First record of sea urchin-associated Epizoanthus planus from Japanese waters and its morphology and molecular phylogeny. Plankon Benthos Res 13(3):136–141

Kise H, Obuchi M, Reimer JD (2021) A new Antipathozoanthus species (Cnidaria, Hexacorallia, Zoantharia) from the northwest Pacific Ocean. ZooKeys 1040:49

Kise H, Santos MEA, Fourreau CJL, Iguchi A, Goto R, Reimer JD (2023) Evolutionary patterns of host switching, lifestyle mode, and the diversification history in symbiotic zoantharians. Mol Phylogenet Evol 182:107732

Krishna Krishnamurthy P, Francis RA (2012) A critical review on the utility of DNA barcoding in biodiversity conservation. Biodivers Conserv 21:1901–1919

Letunic I, Bork P (2021) Interactive Tree Of Life (iTOL) v5: an online tool for phylogenetic tree display and annotation. Nucleic Acids Res 49(W1):W293–W296

McFadden CS, Benayahu Y, Pante E, Thoma JN, Nevarez PA, France SC (2011) Limitations of mitochondrial gene barcoding in Octocorallia. Mol Ecol Resour 11(1):19–31

McMurrich JP (1904) The actiniae of the plate collection. Zool Jahrb 6(Suppl2):215–306 (page(s): 298-299)

Miller MA, Schwartz T, Pfeiffer W (2013) Embedding CIPRES science gateway capabilities in phylogenetics software environments. In: Proceedings of the Conference on Extreme Science and Engineering Discovery Environment: Gateway to Discovery, pp 1–8

Montenegro J, Santos HBW, ME, Kise H and Reimer JD, (2020) Zoantharia (Cnidaria: Hexacorallia) of the Dutch Caribbean and one new species of Parazoanthus. Diversity 12(5):190

Ocaña A, Sánchez Tocino L, López-González PJ (2000) Consideraciones faunísticas y biogeográficas de los antozoos (Cnidaria: Anthozoa) de la costa de Granada (Mar de Alborán). Zool Baetica 11:51–65

Ocaña O, Brito A (2004) A review of Gerardiidae (Anthozoa: Zoantharia) from the Macaronesian islands and the Mediterranean Sea with the description of a new species. Rev Acad Canar Cienc 15(3–4):159–189

Ocaña O, Çinar ME (2018) Descriptions of two new genera, six new species and three new records of Anthozoa (Cnidaria) from the Sea of Marmara. J Nat Hist 52(35–36):2243–2282

Ocaña O, de Matos V, Aguilar R, García S, Brito A (2017) Illustrated catalogue of cold water corals (Cnidaria: Anthozoa) from Alboran basin and North Eastern Atlantic submarine mountains, collected in Oceana campaigns. Rev Acad Canar Cienc 29:221–256

Ocaña O, Moro L, Herrera R, Ertan M, Brito A, Cuervo JS, Herrero R (2019) Parazoanthus axinellae: a species complex showing different ecological requierements. Rev Acad Canar Cienc 31:1–24

Pax F (1937a) Die Korallenfauna der Adria. Teil 1: Krustenanemonen. Thalassia 2(7):3–66

Pax F (1937b) Parazoanthus axinellae als Hohlenbewohner. Note dell'Instituto Italo-Germanico di biologia marina di Rovigno d'Istria 2(5):3–15

Pax F (1957) Die Zoanthanen des Golfes von Neapel. Pubbl Stn Zool Napoli 30:309–329

Poliseno A, Santos MEA, Kise H, Macdonald B, Quattrini AM, McFadden CS, Reimer JD (2020) Evolutionary implications of analyses of complete mitochondrial genomes across order Zoantharia (Cnidaria: Hexacorallia). J Zool Syst Evol Res 58(4):858–868

Quattrini AM, Herrera S, Adams JM, Grinyó J, Allcock AL, Shuler A, McFadden CS et al (2022) Phylogeography of Paramuricea: the role of depth and water mass in the evolution and distribution of deep-sea corals. Front Mar Sci 9:849402

Ramírez-Portilla C, Baird AH, Cowman PF, Quattrini AM, Harii S, Sinniger F, Flot JF (2022) Solving the coral species delimitation conundrum. Syst Biol 71(2):461–475

Reimer JD, Todd PA (2009) Preliminary molecular examination of zooxanthellate zoanthid (Hexacorallia, Zoantharia) and associated zooxanthellae (Symbiodinium spp.) diversity in Singapore. Raffles Bull Zool 22:103–120

Reimer JD, Ono S, Iwama A, Takishita K, Tsukahara J, Maruyama T (2006) Morphological and molecular revision of Zoanthus (Anthozoa: Hexacorallia) from southwestern Japan, with descriptions of two new species. Zoolog Sci 23(3):261–275

Reimer J, Fujii T (2010) Four new species and one new genus of zoanthids (Cnidaria, Hexacorallia) from the Galápagos Islands. ZooKeys 42:1–36

Reimer JD, Sinniger F (2024) World list of Zoantharia. Parazoanthidae Delage and Hérouard, 1901. Accessed through: World Register of Marine Species at: https://www.marinespecies.org/aphia.php?p=taxdetailsandid=100689 on 2024–08–05

Ryland JS, Lancaster JE (2004) A review of zoanthid nematocyst types and their population structure. Hydrobiologia 530:179–187

Santos MEA, Kitahara MV, Lindner A, Reimer JD (2016) Overview of the order Zoantharia (Cnidaria: Anthozoa) in Brazil. Mar Biodivers 46:547–559

Schmidt H (1972) Prodromus zu einer Monographie der mediterranen Aktinien. Zoologica 42:1–121

Schmidt O (1862) Die spongien des adriatischen meeres. W. Engelmann

Shearer TL, Van Oppen MJH, Romano SL, Wörheide G (2002) Slow mitochondrial DNA sequence evolution in the Anthozoa (Cnidaria). Mol Ecol 11(12):2475–2487

Sinniger F, Häussermann V (2009) Zoanthids (Cnidaria: Hexacorallia: Zoantharia) from shallow waters of the southern Chilean fjord region, with descriptions of a new genus and two new species. Org Divers Evol 9(1):23–36

Sinniger F, Chevaldonné P, Pawlowski J (2007) Mitochondrial genome of Savalia savaglia (Cnidaria, Hexacorallia) and early metazoan phylogeny. J Mol Evol 64:196–203

Sinniger F, Montoya-Burgos JI, Chevaldonné P, Pawlowski J (2005) Phylogeny of the order Zoantharia (Anthozoa, Hexacorallia) based on the mitochondrial ribosomal genes. Mar Biol 147:1121–1128

Sinniger F, Ocana OV, Baco AR (2013) Diversity of zoanthids (Anthozoa: Hexacorallia) on Hawaiian seamounts: description of the Hawaiian gold coral and additional zoanthids. PLoS ONE 8(1):e52607

Sinniger F, Reimer JD, Pawlowski J (2008) Potential of DNA sequences to identify zoanthids (Cnidaria: Zoantharia). Zoolog Sci 25(12):1253–1260

Sinniger F, Reimer JD, Pawlowski J (2010) The Parazoanthidae (Hexacorallia: Zoantharia) DNA taxonomy: description of two new genera. Mar Biodivers 40:57–70

Swain TD (2018) Revisiting the phylogeny of Zoanthidea (Cnidaria: Anthozoa): staggered alignment of hypervariable sequences improves species tree inference. Mol Phylogenet Evol 118:1–12

Swain TD, Swain LM (2014) Molecular parataxonomy as taxon description: examples from recently named Zoanthidea (Cnidaria: Anthozoa) with revision based on serial histology of microanatomy. Zootaxa 3796(1):81–107

Terzin M, Villamor A, Marincich L, Matterson K, Paletta MG, Bertuccio V, Bavestrello G, Benedetti Cecchi L, Boscari E, Cerrano C, Chimienti G, Congiu L, Fraschetti S, Mastrototaro F, Ponti M, Sandulli R, Turicchia E, Zane L, Abbiati M, Costantini F (2024) 2bRAD reveals fine-scale genetic structuring among populations within the Mediterranean zoanthid Parazoanthus axinellae (Schmidt, 1862). Coral Reefs, pp 1–14.

Villamor A, Signorini LF, Costantini F, Terzin M, Abbiati M (2020) Evidence of genetic isolation between two Mediterranean morphotypes of Parazoanthus axinellae. Sci Rep 10(1):13938

White TJ, Bruns T, Lee S, Taylor J (1990) Amplification and direct sequencing of fungal ribosomal RNA genes for phylogenetics. PCR Protocols: a Guide to Methods and Applications 18(1):315–322